1997

Single-Frequency, Thin-Film-Tuned, 0.6W, Diode-Pumped Nd:YVO_4 Laser

Jan K. Jabcyński
Military University of Technology

Igor I. Peshko
Wilfrid Laurier University, ipeshko@wlu.ca

Józef Firak
Military University of Technology

Single-frequency, thin-film-tuned, 0.6-W, diode-pumped Nd:YVO_4 laser

Jan K. Jabczyński, Igor I. Peshko, and Józef Firak

Application of a metallic thin-film selector to the single-frequency oscillation of a diode-pumped Nd:YVO_4 laser has been investigated theoretically and experimentally. We show that a chromium thin-film selector with a thickness between 8 and 9 nm provides single-frequency output within a power range of 0.6 W. Single-frequency operation, slow smooth tuning, or chirping was realized by the output coupler movement with a piezoceramic transducer. Chirping at a repetition rate of 0.5 kHz in the 0.5–10-GHz range was achieved. Physical and technical limitations caused by the wide-gain bandwidth, thermal effects, and mechanical vibrations of cavity elements are discussed.

Key words: Diode-pumped lasers, single frequency, frequency tuning, metallic thin-film selector.

1. Introduction

Single-longitudinal-mode laser output is desired for numerous applications such as high resolution spectroscopy, holography, injection seeding, frequency mixing, and optical radar. Resurgence of the solid-state laser has resulted in considerable simplification and compactness of laser devices owing to new laser diode pump systems and new high-doped gain media. In recent years several methods of single-frequency operation in diode-pumped lasers have been demonstrated as follows: nonplanar ring cavity,[1] microchip with a linear cavity,[2,3] gain medium with hole burning,[4] twisting mode cavity,[5] acousto-optically induced feedback,[6] cavity with mode selectors,[7–10] and coupled resonators.[11]

Among these systems the microchip with a linear cavity is the simplest design and has the best mechanical stability. Unfortunately, it also has a high degree of temperature sensitivity to output frequency (several gigahertz per degree). The main source of thermal instability in such lasers is the change of heat dissipation in the gain medium because of technical and physical variations of the pump intensity. The cavity of a microchip is made so short that the cavity mode spacing is greater than the gain bandwidth, and only a single cavity mode can oscillate. Low absorption efficiency of typical butt-coupled diode-pumped Nd:YAG microchips limits the maximum of the cw single-frequency output power to approximately 100 mW. Above this value multimode generation begins as a result of spatial hole burning. For a Nd:$LaSc_3(BO_3)_4$ microchip,[3] approximately 180 mW of single-frequency output power was demonstrated at a temperature of 77 K; however, it decreased to approximately 90 mW at room temperature. A laser with several millimeters of long gain crystal provides approximately 1 W of output power but several modes fall under the gain profile of the active medium. Moreover some attractive active media (such as Nd:YLF, for example) cannot be used in a microchip configuration because of its relatively long absorption length, wide gain bandwidth, or negative thermal dispersion. For a laser with an external cavity, thermal distortion of the gain medium is identical to that for a microchip laser. However, the temperature sensitivity of the frequency connected to the heat dissipation is many times less because of less relative thermal elongation of the cavity.

For a thin crystal the spatial hole burning effect can ensure single-frequency laser operation, especially if the laser has an external cavity and the gain medium is located at the cavity end.[4] However at high pump power and for a relatively wide gain profile some modes or mode groups appear in the generation spectrum. Thus such a laser needs an

J. Jabczyński and J. Firak are with the Institute of Optoelectronics, Military University of Technology, 2 Kaliski Street, 01-489 Warsaw, Poland. I. Peshko is with the Institute of Physics, National Academy of Sciences of the Ukraine, 46 Science Avenue, 252650 Kiev, Ukraine.

Received 1 May 1996; revised manuscript received 3 September 1996.

0003-6935/97/122484-07$10.00/0

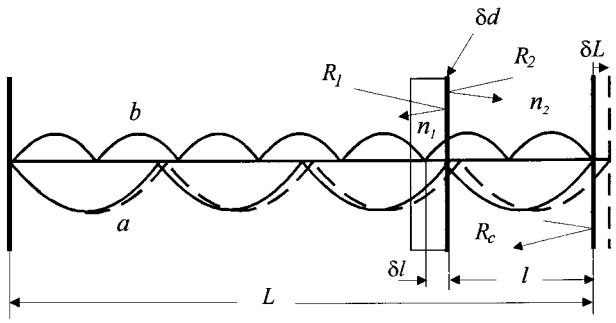

Fig. 1. Scheme of the cavity with an absorbing thin film: a, selected and tuned mode; b, suppressed mode.

additional selector, which can be a metallic thin film placed in the linear cavity.[9,12,13]

2. Metallic Thin-Film Selector and Interferometer with Absorbing Mirror

The principle of metallic thin-film (MTF) selector operation (see Fig. 1) is as follows[12]: The thickness of the MTF δd must be significantly smaller ($\sim\lambda/100$) than the standing wave period. The mode with a node at the MTF location has low loss, whereas the other modes experience higher losses that prevent oscillation. Tuning of the laser output frequency can be realized by mechanical displacement of the MTF from one node to another or by optical change of the cavity length by means of, e.g., an electro-optic effect. Consequently the maximum possible repetition rate of frequency chirping would be some tens of kilohertz (and even a few megahertz for piezoceramic transducer resonance) for the first above mentioned case and hundreds of megahertz for the second.

The MTF selector has been used mainly in a He–Ne laser, which is the system with a narrow gain bandwidth, low output power, and with a relatively high thermal and mechanical stability. The attempts to apply the selector for lamp-pumped solid-state lasers have been unsuccessful. The diode-pumped solid-state lasers have good mechanical stability and a many times broader gain bandwidth than do the He–Ne lasers. For a few millimeters long cavity the fundamental mode diameter is approximately some hundreds of micrometers. Consequently the power density in the cavity can be greater than 10^4 W/cm^2. Thus the possibility of an absorbing selector operation in such conditions had to be proved.

To provide sufficiently sharp selectivity of the MTF selector, the selector should be located in a cavity of length L, where distance δl between the nodes of neighboring modes is greater than the thin-film thickness δd, even though $\delta l = \lambda l/2L > \delta d$ must be satisfied. Here l is the distance between the cavity mirror and the thin film (Fig. 1). On the other hand the selector cannot be placed in the cavity area where the node coincides with different modes. This limits $l < L/N$, where N is the mode number under the whole gain bandwidth.

Table 1. Parameters of Thin-Film Selectors

Chromium Thin-Film Thickness δd (nm)	Reflection from the Substrate Side R_1 (%)	Reflection from the Air Side R_2 (%)	Transmission T (%)
6	3.4	5	81
9	2.5	7.8	68.5
10.5	2	18	58.5

The gain bandwidth of Nd:YVO_4 is approximately 210 GHz. A conventional diode-pumped laser with 2–3-GHz mode spacing can be used to operate 70–100 longitudinal modes. With such a value of N, δl becomes close to or even less than the value of δd. The loss difference for modes with such close node locations is near a few tenths percent,[13] which is sufficient for mode selection in a laser that functions slightly over threshold. However, a pure MTF selector cannot provide precise mode selection at higher pump levels. To control experimentally the selective properties of the pure absorbing selector we manufactured chromium thin film with antireflecting dielectric layers and with a total transmission of approximately 0.8. The single-frequency operation with such a selector has been observed in the pump range of 5% over threshold only, so the output power was approximately a few tens of milliwatts, which is comparable with the results from a typical microchip. To achieve higher output power one should use special properties of a reflective interferometer formed by a MTF selector as well as an output coupler (OC). It is known (see, e.g., Ref. 14) that the reflective interferometer with a metallic mirror has a backreflected spectrum inverse to that of a traditional Fabry–Perot étalon, namely, it consists of bright lines on a black field because of the absence of (or minimized) high reflection from the substrate–film boundary.

The model of the conductive surface can be applied to the thin-film selector[14] if $\delta d \ll \lambda$. When the wave conductivity of substrate n_1 is equal to surface conductivity of the thin film ξ, there is no wave reflection ($R_1 = 0$) from the substrate side of the selector. The simplest experimental situation can be realized for metals that have an imaginary part of conductivity (ξ'') close to zero. In this case the real part ξ' is proportional to the film thickness δd and it is easy to determine δd provided that $R_1 = 0$. In our experiments the chromium thin film deposited onto the fused silica substrate has been used as the selector. Some selectors of different thicknesses have been prepared and investigated. Table 1 lists the reflectivity from both the substrate side (R_1) and the air side (R_2) versus thin-film thickness.

An interferometer placed in the laser cavity disturbs the mode spectrum. A high-finesse interferometer causes an increase of photon lifetime in the cavity, which is equivalent to elongation of the cavity. It has been shown theoretically and experimentally[15]

that the laser cavity with 23-MHz mode spacing demonstrates 18-MHz spacing with the Fox–Smith interferometer located in the cavity. Such an effect leads to a shortening of the distance between nodes on the cavity axis, which is a negative effect from a thin-film selectivity point of view. The backreflective interferometer consisting of a MTF selector and OC should have high finesse but does not necessarily disturb the laser mode spectrum, although it can be adjusted to the cavity axis.

The growth of film thickness leads to an increase of R_2/R_1 (see Table 1), which is a potential improvement of the finesse of the MTF OC interferometer, but a simultaneous increase of absorption losses. This effect decreases the efficiency of single-frequency operation and lowers the finesse of the interferometer. These opposing processes can be effective to stabilize finesse in a specific range of MTF thickness changes. Another problem is the OC transmission optimization. From the best selectivity point of view the less OC transmission, the higher the interferometer finesse. In contrast, the best slope efficiency and maximum multimode output power were achieved experimentally for an OC reflection of approximately 0.9. To optimize the MTF OC interferometer parameters we investigated the interferometer behavior versus MTF thickness and OC transmission.

Based on the principles of multibeam interferometer theory[14] one can obtain an expression for the backreflection of a thin-film-coupler interferometer:

$$R = \frac{A_- + E\sin(2\psi) + F_-\sin^2(\psi)}{A_+ + E\sin(2\psi) + F_+\sin^2(\psi)}, \qquad (1)$$

where $A_\pm = (K \pm KG \pm H)^2 + (KB)^2$, $E = BH(K^2 - 1)$, $F_\pm = (1 \pm G \pm HG)^2 - A_\pm + B^2$, $K = (1 - \sqrt{R_c})/(1 + \sqrt{R_c}) = (1 - R_c^{1/2})/(1 + R_c^{1/2})$, $G = \xi'/n_1$, $B = \xi''/n_1$, $H = n_2/n_1$, R_c is the OC reflection coefficient, n_1 is the refractive index of the substrate, n_2 is the refractive index of the surrounding medium, and $\psi = 2\pi l/\lambda$. Asymmetry of the reflection peak is connected to parameter E. For metals with $\xi'' = 0$ ($E = 0$), the expression for R becomes similar to that of a classic Fabry–Perot interferometer:

$$R = \frac{A_-/A_+ + (F_-/A_+)\sin^2\psi}{1 + (F_+/A_+)\sin^2\psi}. \qquad (2)$$

Coefficient F_+/A_+ can be interpreted as the finesse of the interferometer. For $R_c \to 1$,

$$F_+/A_+ \to \frac{(n_1 + \xi')^2}{n_2^2} - 1. \qquad (3)$$

For the fused silica substrate $n_1 = 1.46$ and for 10.5-nm-thick chromium thin film $\xi' \approx 0.6$. For such parameters the finesse $F_+/A_+ \approx 3.4$. A better way to increase finesse is reduction of the n_2 effective value by dielectric layers deposited onto the thin film. Surface conductivity ξ can be estimated from the volume parameters of the metal, namely, from refractive index n and absorption coefficient χ by classical Drude formulas [$\xi' = 4\pi\chi n\delta d/\lambda$; $\xi'' = 2\pi(n^2 - \chi^2)\delta d/\lambda$]. However, the model of the complex conductive surface provides the possibility for one to calculate ξ' from the optical parameters of the thin film: $\xi' = n_1(1 - T - R_2)/T$. For the calculations we used the experimental values of the thin-film transmission and both side reflections.

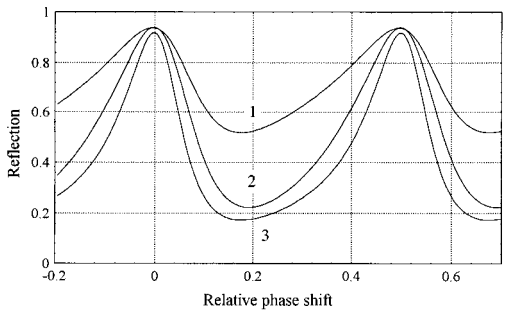

Fig. 2. Reflected spectrum of the MTF OC interferometer with an OC reflection of 0.95 and MTF thicknesses of 1, 6 nm; 2, 9 nm; 3, 10.5 nm.

Figures 2 and 3 demonstrate the calculated interferometer spectra versus a phase shift for different thin-film and OC transmissions. The calculations show that a 9-nm-thick film gives the same reflection maximum as a 6-nm-thick film, but the interferometer spectrum has better contrast and better finesse. It seems that an increase of R_{max} as a result of finesse improvement is compensated by an R_{max} decrease because of higher absorption. For the 10.5-nm film thickness R_{max} decreases although the finesse continues to improve. The changes of the OC transmission for 9-nm-thick film influence R_{max} only and causes almost no change in finesse (Fig. 3). To fulfill all the optimization demands for the preliminary experiments we selected the interferometer elements with the following parameters: chromium thin film with a thickness of approximately 9 nm and an OC with 0.95 reflection.

3. Single-Frequency Laser Operation

The scheme of the laser is shown in Fig. 4. The pump was provided by a 2-W laser diode (LDT-270004). The beam enters into the 1-mm Nd:YVO_4

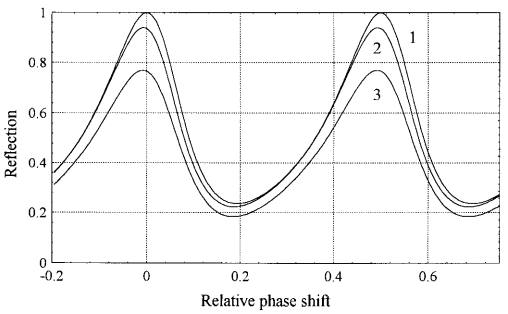

Fig. 3. Reflected spectrum of the MTF OC interferometer with an OC reflection of 1, 0.99; 2, 0.95; 3, 0.8 and a MTF thickness of 9 nm.

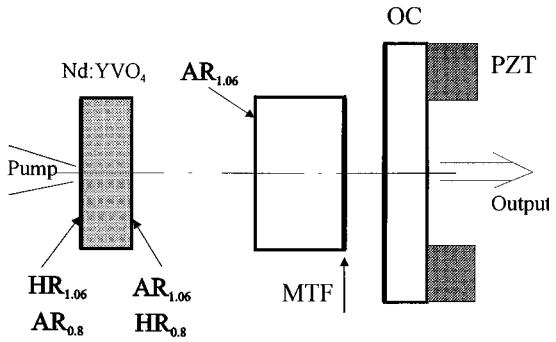

Fig. 4. Laser scheme: Nd:YVO_4, gain crystal; PZT, piezoceramic transducer; MTF, metallic thin film; OC, output coupler; AR, antireflecting coating; HR, high reflecting coating.

crystal through a dichroic coating on the end with 90% transmission at 0.81 μm and 99.5% reflection at 1.06 μm. The internal end of the crystal had an antireflecting coating of 1.06 μm and high reflection coating of 0.8 μm. The chromium thin-film selector was deposited onto a 6-mm-thick fused silica flat–flat plate. The tuning was realized by coupler motion with the piezoceramic transducer along the $\lambda/2$ distance. The total optical length of the cavity was near 6 cm, with a resulting mode spacing of 2.5 GHz. For spectrum review the Fabry–Perot interferometer (IT 28-30) was used with a finesse of 30 and several spacers equivalent to free spectral ranges of 6, 37.5, 150, and 250 GHz. The near-field distribution and the interferometer spectrum images were examined with CCD cameras.

To design the single-frequency laser cavity, first the parameters of multimode laser operation were measured. A maximum of 0.72 W of output power and a slope efficiency of 45% were achieved in the flat cavity with a 5% OC transmission (see Fig. 5). Single-frequency generation was observed to be only slightly above threshold with a maximum output power of approximately 20 mW. For higher pump levels we demonstrated multimode spectrum with some modes separated by 57 and 114 GHz spacing. At a maximum pump power we obtained three or four modes over the gain profile. These frequency intervals correspond to single and double round trips of the emission inside the gain crystal. It has been

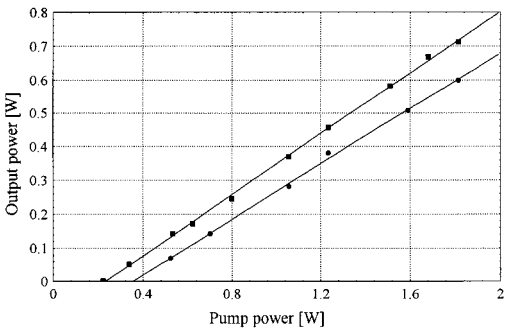

Fig. 5. Output power versus pump power for multimode (rectangles) and single-frequency (circles) mode of operation.

shown[11] that a one uncoated facet Nd:YVO_4 crystal and a 95% reflecting output coupler formed two coupled cavities and gave total reflection modulation at near 8% depth. An antireflection-coated facet on the internal end of our crystal was not ideal and it gave near 2% reflection at 1.06 μm. It seems that the initial mode selection was caused by the crystal surface reflection. The finesse of such an interferometer is not high, but the hole burning effect[3] probably emphasizes the selective properties of the crystal.

The base of the MTF OC interferometer must be able to provide one peak of interferometer transmission over the actual gain spectral range for the maximum pump power, which means that the interferometer base must be less than 1 mm. The initial mode selection makes this demand less stringent. The free spectral range of the interferometer should not be equal to intervals between the naturally selected modes. To fulfill these conditions we chose a 60-mm cavity length and a 3-mm interferometer base.

The single-frequency operation in the flat cavity with a MTF selector placed at a 3 mm distance from the 5% transmission OC has been observed within the complete available pump range (Fig. 5). A maximum output power of 600 mW was achieved that consisted of 85% of the total multimode power at high pump power. A slope efficiency of approximately 41% single-frequency oscillation has been demonstrated. Precise tuning to the maximum of output power at different pump power levels was achieved with MTF displacement by the piezoceramic transducer.

4. Spectrum Tuning

During the tuning process successful thin-film operation can be achieved if permanent coincidence of the node and the selector surfaces is achieved. For mirror displacement δL the corresponding selector displacement should be $\sim\delta L(1 - l/L)$ if the thin film were placed at distance l from the movable mirror (Fig. 1). To simplify the laser design in our experiments we used only the coupler motion. Because of different relative nodes and thin-film speeds the space interval of coincident positions was limited, even though it was quite sufficient for many applications. In the vicinity of the thin film the nodes of neighboring modes were separated by $\lambda l/(2L)$ distances. Consequently, the minimum range of smooth single-frequency tuning is possible inside $\pm\lambda l/(2L)$ limits of the selected mode node position. Such elongation of the standing wave periods corresponds to the frequency change $\Delta\nu = c/[L(L/l - 1)]$. To achieve a wider tuning range one must increase l and decrease L. Smooth tuning is actually possible in the range where amplification is above threshold for some range of frequencies in the vicinity of the interferometer peak.

Figure 6 demonstrates the examples of tuned spectrum for the slow manual changes of the piezotransducer feeding voltage. A smooth tunable range of approximately 0.6 GHz versus 10 V of the feeding voltage has been achieved. According to these estima-

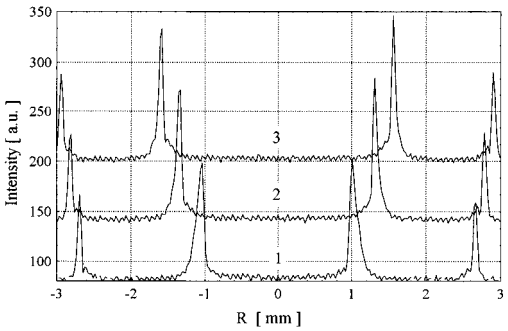

Fig. 6. Examples of the Fabry–Perot interferograms of the laser output versus piezoceramic feeding voltage: 1, 0 V; 2, 4 V; 3, 8 V.

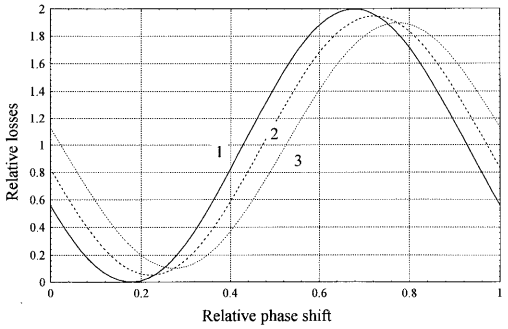

Fig. 7. Relative losses for modes with a transverse index: 2, $\alpha = 0$ and 3, $\alpha = 1$ in the 60-mm-long cavity with a thermal lens and a Rayleigh range of 150 mm; 1, the losses for these modes in the plate–plate cavity.

tions the tuning range for a 60-mm cavity length and a 3-mm interferometer base would be near 0.25 GHz. An experimental tuning range that doubles in width confirms that a high quality mode does not exist in the vicinity of the selected mode. Mode hopping between the lines of the initial nonselected spectrum was observed to change the feeding voltage in the 30-V range.

To achieve a wider smooth tuning range we reduced the cavity length. In this case the cavity consisted of two elements only. The OC was deposited on the external surface of the fused silica plate and the thin film was placed on the internal end. The plate was located as near as possible to the gain crystal. The total cavity length was 8 mm with a resulting cavity mode spacing of 12 GHz. The smooth slow frequency tuning was observed in the 10–15-GHz range depending on the thermal conditions of the crystal. For a cooled or heated crystal thermal elongation had the opposite sign and a natural mode motion was added to or subtracted from the interferometer, reflecting a peak tuning process. For a relatively fast (0.5 kHz) and triangular modulated transducer feeding voltage, we observed a 4–6 GHz chirp for different modes.

5. Thermal Effects

The thermal problems of such lasers concern the active medium as well as the MTF selector. The main thermal effect consists in changing the standing wave figure inside the cavity that is caused by thermal linear expansion and thermal dispersion of the active medium. Moreover, the thermal lensing and thermally induced wave-front aberration affect the quality of single-frequency operation and can even cause damage to the MTF selector. It is well known that, in a microchip laser, thermal lensing takes place even at low pump power levels.[16] Thermal conductivity of YVO_4 crystal is approximately two and a half times less than that of a YAG crystal. Thus the thermal effects must be more striking for a YVO_4 laser.[17,18] Consequently, the Rayleigh range of cavity changes are dependent on the pump power. It has been shown[18] that, for the same YVO_4 crystal as was used in our experiments, at 2-W pump power a thermal lens had approximately 2.5-m^{-1} refractive power. Because of thermal lensing and thermal aberrations generated in the active medium, the distorted wave front and the MTF plane do not coincide. This effect increases the losses for selected modes. On the other hand, the difference between the spaces of transverse mode locations becomes more obvious and a relatively minimum loss can be achieved not only for longitudinal modes but also for higher transverse modes. Following the method proposed in Ref. 19 we calculated the losses for any mode in our experimental conditions. This value can be represented as a relation of the energy absorbed by the thin film to the total energy of one period of the standing wave:

$$\eta = \frac{\iiint_{\nu_{\text{thin film}}} |E|^2[1 - \exp(-\vartheta\delta d)]\mathrm{d}x\mathrm{d}y\mathrm{d}z}{\iiint_{\nu_{\text{mode}}} |E|^2\mathrm{d}x\mathrm{d}y\mathrm{d}z}, \quad (4)$$

where ϑ is the absorption coefficient. The amplitude of any mode $E_{n,m,\alpha}(r, z)$ as a function of radius r and the distance from waist z can be found as a solution of the scalar paraxial wave equation[20]:

$$E_{n,m,\alpha}(r, z) = (1/w)(r/w)^{\alpha}\cos(\alpha\theta)L_m{}^{\alpha}(2r^2/w^2) \times \exp(-r^2/w^2) \times \cos[(2m + \alpha + 1) \times \arctan(z/Z_R) - kr^2/2R_{\text{cur}} - kr^2)], \quad (5)$$

where $L_m{}^{\alpha}$ is the Laguerre polynomial of m radial and α numbers, n is the longitudinal index, w is the beam radius at a distance z from the waist, Z_R is the Rayleigh range, R_{cur} is the radius of curvature of the wave front, and k is the wave number. For the plane MTF and $m = 0$ the final expression for losses of the $\eta_{0,\alpha}(0, \alpha)$ mode is as follows:

$$\eta_{0,\alpha} = (2\delta d/\lambda)[1 - \exp(-\vartheta\delta d)] \times \left\{1 + \frac{\cos[(\alpha + 1)\arctan(z/Z_R) - 2kz]}{[1 + (z/Z_R)^2]^{(\alpha+1)/2}}\right\}. \quad (6)$$

Figure 7 demonstrates the relative losses for the

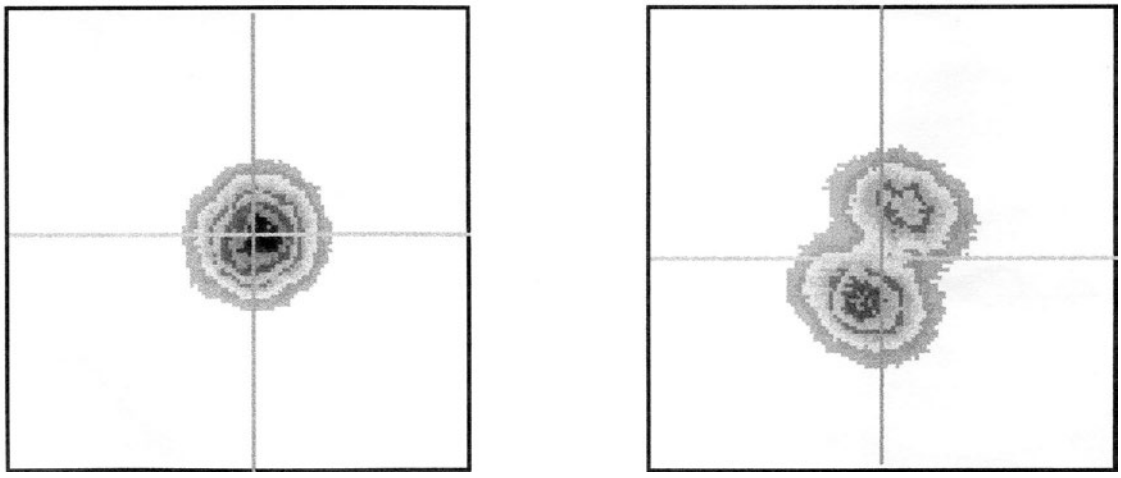

Fig. 8. Far-field intensity distributions of the laser beam for two MTF positions separated by a distance of 13 nm.

fundamental mode and for the transverse mode with $\alpha = 1$ versus the thin-film position in $\lambda/2$ limits. It is evident that, for some selector positions, the transverse mode losses become lower than for the longitudinal mode. For the plate–plate cavity there is almost no difference between the losses of different modes (curve 1). The frequency position of the MTF OC interferometer reflection peak corresponds to the loss minimum. As was mentioned above the selection took place even when there was a small loss difference for the modes in the thin-film selector.

The effect of spatial mode tuning was observed experimentally for a pump power greater than 1.5 W. Figure 8 shows two examples of the output intensity distribution for the selector position difference of approximately 13 nm or approximately 1.5-V feeding voltage difference in the piezoceramic transducer. The modes of higher transverse index were not observed probably because of the natural transverse selection by the small size pump excited area in the gain medium and because of higher absorption losses in the selector (Fig. 7).

The laser with a 10.5-nm-thick MTF selector demonstrated approximately 420 mW of output power only. At a pump power higher than 1.5–1.6 W the output power begins to decrease. However the better power stability of single-frequency operation and less sensitivity to mechanical noises was observed for such a selector. The absorption increase and diffraction losses of the MTF OC interferometer decreased the total efficiency of single-frequency operation in this case.

6. Technical Limitations

It was mentioned above that the thin-film thickness is approximately $\lambda/100$. Consequently, the optical surfaces of laser elements should have the same tolerance across a laser beam. Otherwise there is no good coincidence between the standing wave node position and the thin film. Thus a decrease of interferometer finesse and an increase of absorption in the thin film would take place, which can be the reason for film damage.

A typical length of a laser cavity is approximately a few centimeters. The coefficient of relative thermal expansion of the cavity base materials is usually approximately 10^{-5}. The cavity length thermal sensitivity is between approximately 0.1 and 1 μm/K. So the cavity length changes per degree is 10–50 times greater than the film thickness or distance between the wave nodes along the optical axis in the selector position. This means that minimum thermal stabilization of approximately 10^{-2} K should be provided for successful thin-film operation. The same difficulties are connected with possible mechanical vibrations of mirror holders. Moreover at the moment of fast thermal or mechanical changes of the cavity length or of mirror orientation the maximum intensity of the operating mode passes through the MTF and can damage it. To provide long-term laser operation stability and to prevent MTF damage, thermal and mechanical stabilization is obligatory. In our laboratory conditions without any special stabilization effort but without rough thermal and mechanical noise sources the spontaneous frequency tuning was near 0.3 GHz within a 10-min period.

7. Conclusions

It seems that a diode-pumped microcrystal laser with a relatively short external cavity and thin-film selector accumulates the majority of positive properties of microchip lasers. However it has its own disadvantages and advantages: fast mode hopping or smooth tuning and chirping of single-frequency oscillation can be realized, it provides relatively high output power, it can be stabilized electronically without extensive effort, the driving voltage for the piezoceramic is a few tens of volts, and it is extremely simple and inexpensive to produce.

In summary, we have obtained single-frequency output from a diode-pumped 1-mm-thick Nd:YVO_4 crystal using 6–60-mm cavities with an 8–9-nm-

thick chromium selector. Over 600 mW of the single-frequency output power with a slope efficiency of approximately 41% have been obtained. Transverse mode tuning was observed for pump power greater than 1.5 W. Mode hopping in the 114-GHz range and smooth chirping of between 0.5 and 10 GHz have been realized with a repetition rate of 0.5 kHz.

This research was supported by the Polish Committee for Scientific Research under grant T11B00708. The laser element coatings were made by M. Trnka from COBRABiD-VAC, Poland.

References

1. T. J. Kane and R. L. Byer, "Monolithic, unidirectional, single-mode Nd:YAG ring laser," Opt. Lett. **10,** 65–67 (1985).
2. J. J. Zayhowski and A. Mooradian, "Single frequency microchip Nd:YAG lasers," Opt. Lett. **14,** 24–26 (1989).
3. J. J. Zayhowski, "The effects of spatial hole burning and energy diffusion on the single-mode operation of standing-wave lasers," IEEE J. Quantum Electron. **26,** 2052–2057 (1990).
4. B. Beier, J.-P. Meyn, R. Knappe, K.-J. Boller, G. Huber, and R. Wallenstein, "A 180 mW Nd:$LaSc_3(BO_3)_4$ single-frequency TEM_{00} microchip laser pumped by an injection locked diode-array," Appl. Phys. B **58,** 381–388 (1994).
5. K. Wallmeroth, "Monolithic integrated Nd:YAG laser," Opt. Lett. **15,** 903–905 (1990).
6. W. A. Clarkson and D. C. Hanna, "Acousto-optically induced unidirectional single mode operation of a *Q*-switched miniature Nd:YAG ring laser," Opt. Commun. **81,** 375–378 (1991).
7. S. W. Henderson and C. P. Hale, "Tunable single-longitudinal-mode diode laser pumped Tm:Ho:YAG laser," Appl. Opt. **29,** 1716–1718 (1990).
8. P. Nachman, J. Munch, and R. Yee, "Diode-pumped, frequency-stable, tunable, continuous-wave Nd:glass laser," IEEE J. Quantum Electron. **26,** 317–321 (1990).
9. F. J. Effeenberger and G. J. Dixon, "Gradient-index-mirror solid state lasers," Appl. Opt. **33,** 5537–5541 (1994).
10. P. Laporta, S. Longhi, S. Taccheo, and O. Svelto, "Single-mode cw erbium–ytterbium glass laser in 1.5 μm," Opt. Lett. **18,** 31–33 (1993).
11. C. Pedersen, P. L. Hansen, T. Skettrup, and P. Buchhave, "Diode-pumped single-frequency Nd:YVO_4 laser with a set of coupled resonators," Opt. Lett. **20,** 1389–1391 (1995).
12. Yu. V. Troitskii and N. D. Goldina, "Optical resonator with absorbing film as a mode selector," J. Exp. Theor. Phys. Lett. **7,** 309–313 (1968).
13. A. Belozerov, A. B. Golovin, I. I. Kuratev, I. I. Peshko, A. I. Khiznyak, Yu. V. Tsvetkov, and F. M. Yatsyuk, "The single-frequency stimulated emission from a YAG:Nd^{3+} mini-laser with radiation wavelength tuning," Sov. J. Quantum Electron. **18,** 1180–1182 (1991).
14. Yu. V. Troitskii, *Multibeam Interferometers of Reflected Light* (Nauka, Novosibirsk, 1985), p. 205.
15. E. Nichelatti and G. Salvetti, "Transverse modes in laser cavities terminating in reflective multipass interferometers," Appl. Opt. **34,** 2655–2658 (1995).
16. J. J. Zayhowski, "Thermal guiding in microchip lasers," in *Advanced Solid State Lasers*, Vol. 6 of OSA Proceedings Series (Optical Society of America, Washington, D.C., 1990), pp. 9–13.
17. T. M. Baer and M. S. Keirstead, "Modeling of high power end-pumped solid-state laser," in *Conference on Lasers and Electro-Optics*, Vol. 11 of OSA Technical Digest Series (Optical Society of America, Washington, D.C., 1993), paper CFM1.
18. J. K. Jabczyński and K. Kopczyński, "Thermally induced GRIN effects in diode pumped laser," Opt. Appl. **25,** 301–310 (1995).
19. R. Vodnytskii, A. Dlugasheck, M. Novack, I. Peshko, A. Khizhnyak, Z. Yankievich, and F. Yatsyuk, "A thin-film selector in a spherical cavity," Sov. J. Quantum Electron. **18,** 989–992 (1991).
20. Yu. A. Anan'ev, *Optical Cavities and Laser Emission Divergence Problem* (Nauka, Moscow, 1979).